

## A Supramolecular Host-Guest Carrier System for Growth Factors Employing VHH Fragments

Jordi Cabanas-Danés, Emilie Rodrigues, Ellie Landman, Jasper van Weerd, Clemens A. van Blitterswijk, Theo Verrips, Jurriaan Huskens, Marcel Karperien, and Pascal Jonkheijm

*J. Am. Chem. Soc.*, **Just Accepted Manuscript** • DOI: 10.1021/ja505695w • Publication Date (Web): 25 Aug 2014

Downloaded from <http://pubs.acs.org> on August 27, 2014

### Just Accepted

“Just Accepted” manuscripts have been peer-reviewed and accepted for publication. They are posted online prior to technical editing, formatting for publication and author proofing. The American Chemical Society provides “Just Accepted” as a free service to the research community to expedite the dissemination of scientific material as soon as possible after acceptance. “Just Accepted” manuscripts appear in full in PDF format accompanied by an HTML abstract. “Just Accepted” manuscripts have been fully peer reviewed, but should not be considered the official version of record. They are accessible to all readers and citable by the Digital Object Identifier (DOI®). “Just Accepted” is an optional service offered to authors. Therefore, the “Just Accepted” Web site may not include all articles that will be published in the journal. After a manuscript is technically edited and formatted, it will be removed from the “Just Accepted” Web site and published as an ASAP article. Note that technical editing may introduce minor changes to the manuscript text and/or graphics which could affect content, and all legal disclaimers and ethical guidelines that apply to the journal pertain. ACS cannot be held responsible for errors or consequences arising from the use of information contained in these “Just Accepted” manuscripts.



# A Supramolecular Host-Guest Carrier System for Growth Factors Employing V<sub>H</sub>H Fragments

Jordi Cabanas-Danés,<sup>†</sup> Emilie Dooms Rodrigues,<sup>‡</sup> Ellie Landman,<sup>‡</sup> Jasper van Weerd,<sup>‡,‡</sup> Clemens van Blitterswijk,<sup>‡</sup> Theo Verrips,<sup>§</sup> Jurriaan Huskens,<sup>‡,\*</sup> Marcel Karperien,<sup>‡,\*</sup> Pascal Jonkheijm<sup>‡,\*</sup>

<sup>†</sup>Molecular Nanofabrication Group, MESA<sup>+</sup> Institute for Nanotechnology, Faculty of Science and Technology, University of Twente P.O. Box 217, 7500 AE, Enschede, Netherlands.

<sup>‡</sup>Departments of Developmental Bioengineering and <sup>‡‡</sup>Tissue Regeneration, MIRA Institute for Biomedical Technology and Technical Medicine, Faculty of Science and Technology, University of Twente P.O. Box 217, 7500 AE, Enschede, Netherlands.

<sup>§</sup>Cellular Architecture and Dynamics, Department of Biology, Faculty of Science, Utrecht University, Padualaan 8, 3584 CH, Utrecht, Netherlands.

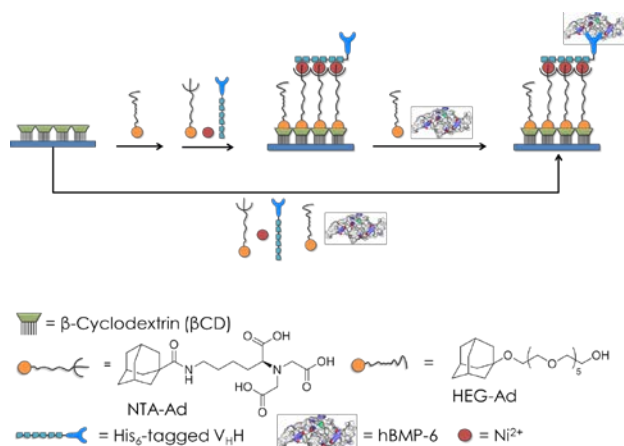
**KEYWORDS.** *Supramolecular chemistry, Delivery, Self-Assembly, Growth Factor, Immobilization.*

**ABSTRACT:** A supramolecular strategy is presented for the assembly of growth factors employing His<sub>6</sub>-tagged single-domain antibodies (V<sub>H</sub>H). A combination of orthogonal supramolecular interactions of β-cyclodextrin (βCD)-adamantyl (Ad) host-guest and N-nitrilotriacetic acid (NTA)-histidine (His) interactions was employed to generate reversible and homogeneous layers of growth factors. A single-domain antibody V<sub>H</sub>H fragment was identified to bind to the human bone morphogenetic protein-6 (hBMP6) growth factor and could be recombinantly expressed in *E. coli*. The V<sub>H</sub>H fragment was equipped with a C-terminal hexahistidine (His<sub>6</sub>) tether to facilitate the assembly on βCD surfaces using a linker that contains an Ad group to bind to the βCD receptors and an NTA moiety to interact with the His<sub>6</sub>-tag upon co-complexation of Ni<sup>2+</sup> ions. After exploring the thermodynamic and kinetic stability of the V<sub>H</sub>H assemblies on βCD surfaces using a variety of experimental techniques including microcontact printing (μCP), surface plasmon resonance (SPR), microscale thermophoresis (MST) and theoretical models for determining the thermodynamic behavior of the system, hBMP6 was assembled onto the V<sub>H</sub>H-functionalized surfaces. After analyzing the immobilized hBMP6 using immunostaining, the biological activity of hBMP6 was demonstrated in cell differentiation experiments. Early osteogenic differentiation was analyzed in terms of alkaline phosphatase (ALP) activity of KS483-4C3 mouse progenitor cells and the results indicated that the reversibly immobilized growth factors were functionally delivered to the cells. In conclusion, the supramolecular strategy used here offers the necessary affinity, reversibility and temporal control to promote biological function of the growth factors that were delivered by this strategy.

Growth factors are considered major therapeutic agents that profoundly affect cell function.<sup>1-6</sup> However, direct bolus delivery or systemic administration of growth factors are of limited clinical use as excessive dosing is required to detect a measurable effect, which potentially could lead to off-target effects.<sup>7</sup> Correct localization and balance of growth factors can be regulated by their encapsulation in carrier systems such as hydrogels, scaffolds or layer-by-layer systems, which generally sustain the spatial availability of growth factors facilitated by their diffusion into tissue.<sup>8-21</sup> An elegant strategy recently reported by Maynard *et al.* relied on the stabilization of basic fibroblast growth factors by covalent conjugation with a heparin-mimicking polymer.<sup>22</sup> Here we report the supramolecular capture of growth factors by using single monomeric variable antibody fragments engineered from heavy chain antibodies found in

camelids (V<sub>H</sub>H fragments). Several therapeutic applications employing V<sub>H</sub>H in cancer, infectious and immune diseases have recently been reviewed.<sup>23-25</sup> Unique characteristics of V<sub>H</sub>H fragments such as their small size (12-20 kDa), elevated stability in aqueous and even in organic solvents and higher temperatures and reproducible recombinant production make them promising candidates to explore for activating surfaces in tissue regeneration. In addition, selection of V<sub>H</sub>H binders to growth factors can be conveniently done by means of phage display. V<sub>H</sub>Hs are amenable for genetic engineering allowing the site-specific introduction of reactive groups, such as histidine tags, through which they can be site-specifically immobilized to surfaces yielding homogeneously oriented layers of V<sub>H</sub>H fragments under physiological conditions following supramolecular strategies.<sup>26, 27</sup>

Supramolecular strategies, similar to bio-responsive covalent linkages such as ester or thiol linkages, yield reversibility providing a means to release growth factors and prompt a biological function directly influenced by the desorption. However as opposed to such type of bio-responsive covalent linkages, supramolecular delivery can be controlled by valency and dissociation rate constants. Although supramolecular chemistry has been successfully used to create biomimetic systems,<sup>28-37</sup> up to now, reports that show the potentialities of supramolecular growth factor delivery systems predominantly employ peptide fragments to allow for binding of growth factors to supramolecular assemblies. For example, Stupp *et al.* have bound transforming growth factor  $\beta$ -1 (TGF- $\beta$ ) to oligopeptides that were displayed on the surface of self-assembled nanotubular systems.<sup>38</sup> Such supramolecular carrier systems promoted chondrogenic differentiation of human mesenchymal stem cells.<sup>38</sup> Up to now promising reports exist on the use of supramolecular host-guest systems, such as cyclodextrin and cucurbituril hosts, for the delivery of transcription factors,<sup>39</sup> for the release of peptides and proteins<sup>40-42</sup> and to modulate cell adhesion,<sup>43-46</sup> however, yet no reports exist for their application as growth factor carrier systems.<sup>11, 28-30, 47</sup>



**Scheme 1. Schemetically Presented Is The Assembly Of hBMP-6 On Supramolecular  $\beta$ CD Host Surfaces. The Self-Assembly Follows Either A Step-wise (Three Steps) Or One-Pot Procedure. See Text For Details. Chemical Structures Of The Building Blocks Are Given At The Bottom.**

We here present a supramolecular strategy to deliver growth factors on  $\beta$ -cyclodextrin ( $\beta$ CD) surfaces using V<sub>H</sub>H as an intermediate. The method requires simple assembly steps in physiological conditions and offers the possibility to fine-tune affinities and dissociation rate constants by molecular design. We demonstrate the feasibility of our approach using human bone morphogenetic protein 6 (hBMP-6) as a model growth factor that is not recombinantly available and therefore

cannot be expressed with His-tags to allow for direct non-covalent immobilization. hBMP-6 belongs to the TGF- $\beta$  superfamily and is known to play significant roles in cartilage and bone morphogenesis and repair and is already used as a therapeutic protein for inducing bone growth.<sup>48-50</sup>

## Results and Discussion

**Design and Characterization of V<sub>H</sub>H Construct.** V<sub>H</sub>H clones that bind to hBMP-6 were selected following a phage display approach (see Supporting Information for details). Affinity selection (biopanning) was carried out on hBMP-6 coated plates (0.2-5  $\mu$ g/well), which were incubated with the phage V<sub>H</sub>H immune library that was constructed after immunization of Llamas. After the second round, the relative binding strength of selected phage V<sub>H</sub>H clones were assessed against each other using an enzyme-linked immunosorbent assay (ELISA) (See Supporting Figure S1a). Subsequently, the strongest binding V<sub>H</sub>H clone was sub-cloned in an expression vector with a C-terminal His-tag and recombinantly produced in *E. Coli* hosts. After purification using affinity chromatography, a single band at 16 kDa was detected by sodium dodecylsulfate-polyacrylamide gel electrophoresis (SDS-PAGE) (See Supporting Figure S1b) in agreement with related V<sub>H</sub>H binders described in literature.<sup>22-25</sup>

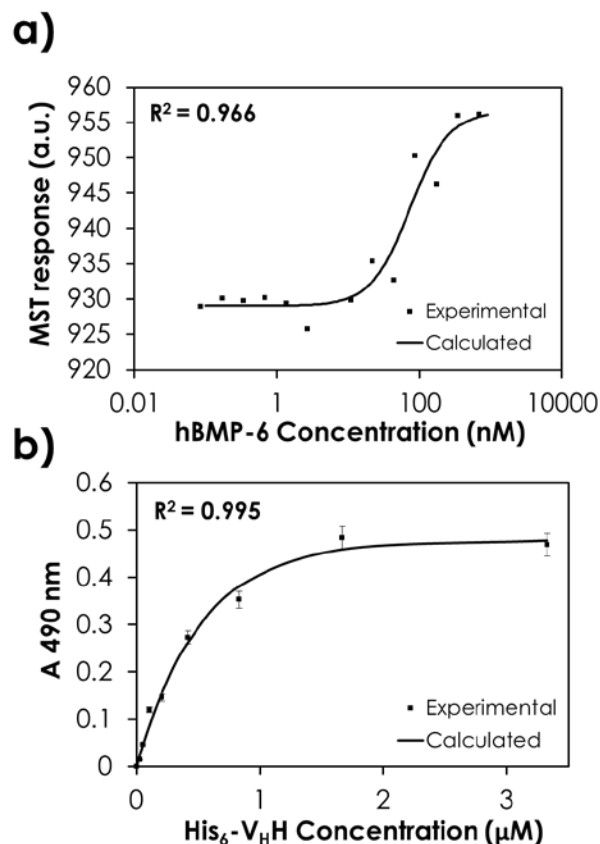


**Figure 1.** V<sub>H</sub>H binding to hBMP-6 analyzed a) in solution by microscale thermophoresis (MST) and b) on microtiter plates by ELISA (duplicate read-out).

The interaction of the purified  $V_{\text{H}}\text{H}$  construct with hBMP-6 was confirmed using microscale thermophoresis (MST) and ELISA measurements. To determine the affinity between  $V_{\text{H}}\text{H}$  and hBMP-6 in solution, MST was used. A titration series of hBMP-6 over a range of 0.04 nM to 0.7  $\mu\text{M}$  was performed while fluorescently labeled  $V_{\text{H}}\text{H}$  was kept constant at 20 nM throughout the series. Upon binding of hBMP-6, a change in thermophoretic signal was observed as shown in Figure 1a.

Subsequent fitting of the data to a 1:1 binding model yielded a dissociation constant  $K_d$  of  $7.4 (\pm 0.4) \times 10^{-8}$  M and therefore  $K_a = 1/K_d = 1.4 \times 10^7$   $\text{M}^{-1}$ . These values are comparable to the ones found in literature for  $V_{\text{H}}\text{H}$  interactions with different binding partners.<sup>22-25, 51-53</sup> The obtained affinity was compared with affinity studies carried out in an ELISA assay format. To the hBMP-6 coated microtiter plates, a series of  $V_{\text{H}}\text{H}$  solutions in the range of 0-3.3  $\mu\text{M}$  was added and assayed by ELISA (Figure 1b). After fitting the experimental data to a Langmuir model, a  $K_a$  of  $1.9 (\pm 0.2) \times 10^6$   $\text{M}^{-1}$  was estimated, which is one order of magnitude lower than the affinity measured by MST, which is a known effect when comparing solution assays with array formats.<sup>26, 27</sup>

**Surface Assembly Analysis.** With these  $V_{\text{H}}\text{H}$  constructs with high affinity towards hBMP-6 in hand, we sought to employ the C-terminal His<sub>6</sub>-tag on the recombinantly produced  $V_{\text{H}}\text{H}$  for the assembly onto supramolecular  $\beta\text{CD}$  host surfaces through specific interaction with adamantyl (Ad) guest functionalized nitrilotri(acetic acid) (NTA) linkers.<sup>54-56</sup> To fabricate this supramolecular carrier system a step-wise assembly process (Scheme 1) was adopted using the (NTA)-Ni(II)-His<sub>6</sub>-tag interaction and orthogonal linkers consisting of three steps, i.e. (1) pre-incubation of the  $\beta\text{CD}$  surface with an ethylene glycol based mono-adamantyl linker (HEG-Ad) for minimizing the non-specific protein adsorption, (2) a solution of NTA-monoadamantyl linker (NTA-Ad) and  $V_{\text{H}}\text{H}$  in the presence of Ni(II) ions while maintaining the same concentration of HEG-Ad and (3) a solution of hBMP-6 was used.<sup>39-40</sup> Alternatively, after assembling HEG-Ad, a one-pot assembly step with all components was performed (Scheme 1). The assembly was performed at a physiological pH of 7.4, which ensures complexation of Ni(II) ions to the majority of the NTA moieties.<sup>50</sup>

Supramolecular  $\beta\text{CD}$  host monolayers on gold were placed in an SPR flow cell.<sup>40</sup> After the baseline became stable while flowing PBS buffer, a solution of HEG-Ad (0.1 mM in PBS) was flown for 10 min until a stable signal was observed (Figure 2a, triangles). Successively, a solution of 0.5  $\mu\text{M}$   $V_{\text{H}}\text{H}\cdot\text{Ni(II)}\cdot\text{NTA-Ad}$  (in a ratio of 1:5:5) in the presence of 0.1 mM HEG-Ad was injected and flown continuously (0.1 mL min<sup>-1</sup>) (Figure 2a, squares). The observed increase in the SPR signal reached thermodynamic equilibrium after 10 min (Figure 2a, spheres). This observation indicates that  $V_{\text{H}}\text{H}\cdot(\text{Ni(II)}\cdot\text{NTA-Ad})_x$  ( $x=1-3$ ) species have replaced monovalent HEG-Ad confirming that higher valent adamantyl  $V_{\text{H}}\text{H}\cdot(\text{Ni(II)}\cdot\text{NTA-Ad})_x$  ( $x>1$ ) were preferentially interacting with the supramolecular  $\beta\text{CD}$

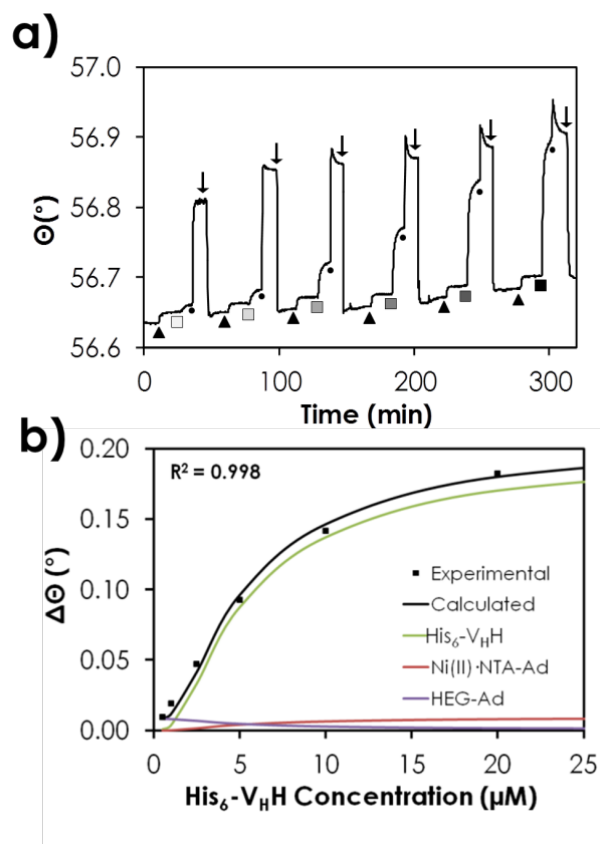


**Figure 2.** A) SPR data of a titration series of  $V_{\text{H}}\text{H}\cdot\text{Ni(II)}\cdot\text{NTA-Ad}$  (1:5:5) to  $\beta\text{CD}$  plates in the presence of 0.1 mM HEG-Ad. Symbols indicate switching of the buffer to: 0.1 mM HEG-Ad ( $\blacktriangle$ ), increasing concentrations of  $V_{\text{H}}\text{H}\cdot\text{Ni(II)}\cdot\text{NTA-Ad}$  (1:5:5;  $\square$ ,  $\blacksquare$ ) in the presence of 0.1 mM HEG-Ad, 10 mM  $\beta\text{CD}/\text{EDTA}$  in PBS ( $\bullet$ ) and PBS ( $\downarrow$ ). B) Experimental change of SPR resonant angle ( $\Delta\theta$  at thermodynamic equilibrium; black markers) versus  $V_{\text{H}}\text{H}$  concentration fitted to the theoretical model (See Supporting Information). The contribution of the assembly of the different molecules to the signal is given.

host surface as determined by the effective concentration ( $C_{\text{eff}}$ ) (*vide infra*). To demonstrate the reversibility of the assembly of  $V_{\text{H}}\text{H}$ , a solution containing 10 mM of competing ligand EDTA and 10 mM of  $\beta\text{CD}$  in PBS were added to the flow cell while monitoring the SPR response (Figure 2a, spheres). Although a sudden initial increase in the SPR intensity was observed due to the large change in refractive index when using a concentrated solution of EDTA and  $\beta\text{CD}$ , the baseline was totally restored upon rinsing the system with PBS for 5 min (Figure 2a, arrows). This result indicates the complete disassembly of the molecules from the  $\beta\text{CD}$  surface. To assess the thermodynamic stability of the  $V_{\text{H}}\text{H}$  constructs at the  $\beta\text{CD}$  surface, a titration series of  $V_{\text{H}}\text{H}\cdot\text{Ni(II)}\cdot\text{NTA-Ad}$  (1:5:5) in the range of 0.5-20  $\mu\text{M}$  was performed while recording the change in the SPR resonant angle. Between each titration step a disassembly cycle was performed to restore the  $\beta\text{CD}$  surface as described above. Upon addition of HEG-Ad, which represents the first step of the

assembly of each titration step, a constant increase in SPR intensity was observed (Figure 2a). The second step of the assembly was marked by a gradual increase in the change of the SPR resonant angle saturating above 20  $\mu\text{M}$  of  $V_{\text{H}}\text{H}$  (Figures 2a and 2b).

The SPR data were satisfactorily fitted to a thermodynamic model that accounts for all species possibly bound to the  $\beta\text{CD}$  surface (Figure 2b, see Supporting Information for details). The model shows that at low concentrations of  $V_{\text{H}}\text{H}$  ( $< 1 \mu\text{M}$ ), the major contribution to the (still low) SPR signal originates from the assembly of monovalent HEG-Ad, while above 2  $\mu\text{M}$  of  $V_{\text{H}}\text{H}$ , when the coverage becomes appreciable, the major contribution to the rise in SPR signal originates from trivalent  $V_{\text{H}}\text{H}\cdot(\text{Ni}(\text{II})\cdot\text{NTA-Ad})_3$  species (70%) as expected.<sup>55</sup> This indicates that the trivalent complex is the main species contributing to the coverage at the whole range of concentrations until surface saturation (See Figure 2b and Supporting Figure S2b). Fixing the values of the intrinsic binding constants  $K_{i,\text{HEG}} = 2.6 \times 10^4 \text{ M}^{-1}$  and  $K_{i,\text{NTA}} = 1.2 \times 10^4 \text{ M}^{-1}$  as found in literature,<sup>51</sup> an association constant  $K_1$  of  $6.3 \times 10^4 \text{ M}^{-1}$ , which represents the first interaction of  $\text{Ni}(\text{II})\cdot\text{NTA-Ad}$  to the  $\text{His}_6$ -tag, and a value for  $C_{\text{eff}}$  of 0.02 M were found to fit the experimentally observed changes in SPR resonant angle (Figure 2b). From these values, the second ( $K_2$ ) and third ( $K_3$ ) association constants of the consecutive bonding of  $\text{His}_2$ -units to  $\text{Ni}(\text{II})\cdot\text{NTA-Ad}$  were calculated to be  $1.5 \times 10^4 \text{ M}^{-1}$  and  $1.95 \times 10^3 \text{ M}^{-1}$  in agreement with values found in literature.<sup>50, 57</sup> The overall binding constant for the trivalent complex on the  $\beta\text{CD}$  surface ( $[V_{\text{H}}\text{H}] = 2 \mu\text{M}$  and  $[\text{Ni}(\text{II})\cdot\text{NTA-Ad}] = 10 \mu\text{M}$ ) was calculated to be in the order of  $10^6 \text{ M}^{-1}$  in agreement with literature<sup>58</sup> and for the divalent complex in the order of  $10^5 \text{ M}^{-1}$ . In both cases, the multivalent interactions lead to highly stable assemblies bound to the surface while still reversible.

**Release of  $V_{\text{H}}\text{H}$  Fragments.** To visualize the release of the  $V_{\text{H}}\text{H}$  carrier system fluorescence microscopy was used. To this end,  $V_{\text{H}}\text{H}$  was first fluorescently labeled with a Cy3-dye following standard procedures (see Supporting Information).  $\text{Cy}_3\text{-}V_{\text{H}}\text{H}$  was used for patterning employing the well-established microcontact printing ( $\mu\text{CP}$ ) method with a polydimethylsiloxane (PDMS) stamp.<sup>40, 59</sup> Such stamps were inked for 2 min with a mixture of 1  $\mu\text{M}$   $\text{Cy}_3\text{-}V_{\text{H}}\text{H}:\text{Ni}(\text{II})\cdot\text{NTA-Ad}$  (1:5:5) in PBS buffer. After inking, the stamp was blown dry and put into conformal contact with a supramolecular host glass surface for 5 min. After removing the stamp, the slides were directly imaged. As a reference, the same experiment was performed in which the PDMS stamp was inked with a 1  $\mu\text{M}$  solution of  $V_{\text{H}}\text{H}$  without  $\text{Ni}(\text{II})\cdot\text{NTA-Ad}$  added. In both cases, uniform dot patterns of 50  $\mu\text{m}$  diameter and spaced by 10  $\mu\text{m}$  were clearly visible with an excellent contrast with the background as imaged using fluorescence microscopy (See Figure 3a and Supporting Figure S3). After extensive rinsing for 30 min with PBS, the patterns disappeared in the case of the reference experiment, which lacked the supramolecular NTA-Ad linker, whereas clear patterns remained visible in the case

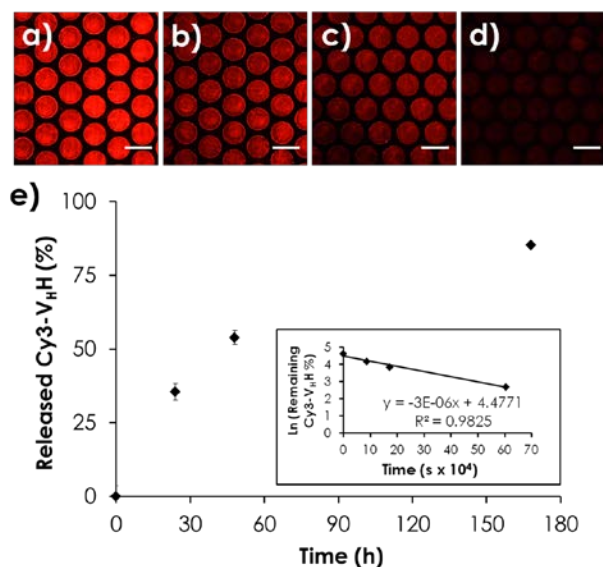


**Figure 3.** a) Fluorescence microscopy image of  $\text{Cy}_3\text{-}V_{\text{H}}\text{H}$  patterned by  $\mu\text{CP}$  on  $\beta\text{CD}$  glass slides recorded immediately after printing and washing. Frames recorded with 0.2 sec exposure time after immersion for b) 24 h, c) 48 h and d) 168 h in cell culture medium. Scale bars indicate 100  $\mu\text{m}$ . e) Release of  $\text{Cy}_3\text{-}V_{\text{H}}\text{H}$  is plotted relative to the initial fluorescence intensity versus logarithmic time. Inset shows the linear fitting of the corresponding logarithmic values.

when NTA-Ad was co-printed (See Supporting Figure S3). These results indicate that the interactions between  $V_{\text{H}}\text{H}$  and the surface are governed by specific NTA- $\text{Ni}(\text{II})\text{-His}_6$ -tag interactions as envisioned. Subsequently, after washing the patterns of the supramolecular  $V_{\text{H}}\text{H}$  carrier system with a solution containing 10 mM of  $\beta\text{CD}$  and EDTA the patterns disappeared (see Supporting Figure S3), which is characteristic of reversible supramolecular interactions between the protein and the surface. The observations made by fluorescence microscopy suggest that homogeneous layers of oriented  $V_{\text{H}}\text{H}$  are fabricated as a result of specific and reversible supramolecular interactions, in agreement with the SPR studies.

To acquire more information about the release of the  $V_{\text{H}}\text{H}$  fragments from the supramolecular  $V_{\text{H}}\text{H}$  carrier system under in vitro conditions, a series of substrates patterned with  $\text{Cy}_3\text{-}V_{\text{H}}\text{H}\cdot\text{Ni}(\text{II})\cdot\text{NTA-Ad}$  were immersed in cell culture medium and four frames were recorded with a 0.2 sec exposure time using an inverted fluorescence microscope (Figure 3a-d). When plotting the decay of the fluorescence intensity versus time (Figure 3e), after 7 days around 80% of the fluorescence of the  $\text{Cy}_3\text{-}V_{\text{H}}\text{H}$  disappeared from the  $\beta\text{CD}$  host surfaces. When the data were fitted with first-order kinetics a dissociation rate constant of  $k_d = \sim 10^{-6} \text{ s}^{-1}$  was found, which compares favorably to an example in literature of immobilizing  $\text{His}_6$ -tagged proteins on covalently modified NTA-surfaces.<sup>60</sup>

**Growth Factor Assembly.** The ability to extend the release of  $V_{\text{H}}\text{H}$  beyond days provides an interesting opportunity to apply our supramolecular carrier system

for the delivery of growth factors to cells. To investigate whether the  $V_{\text{HH}}$  carrier system can be loaded with hBMP-6 growth factors, patterns of dots of  $V_{\text{HH}}$  were fabricated on glass slides as described above and subsequently incubated with a solution containing hBMP-6 ( $0.7 \mu\text{M}$ ) for 1 h, according to the step-wise approach (Scheme 1). After sequential coupling for 1 h of a primary antibody (Ab) specific to hBMP-6 and a FITC-labeled secondary Ab, the slides were imaged using fluorescence microscopy. The recorded images show clearly that the fluorescently labeled antibody was selectively immobilized on the printed  $V_{\text{HH}}$  patterns (Figure 4a). When surfaces were blocked with BSA in addition to HEG-Ad prior to incubating the slides with hBMP-6 and antibodies, the signal-to-noise was enhanced. When the immunoassay was carried out on the  $V_{\text{HH}}$  patterns in the absence of hBMP-6 no fluorescent patterns were observed (Figure 4b). Similar results were obtained when the one-pot procedure was followed. When hBMP-6 loaded surfaces were immersed in cell culture medium, inspection of the surfaces using fluorescence microscopy showed that the disappearance of the growth factor and  $V_{\text{HH}}$  fragments occurred in the same time window as compared to the  $V_{\text{HH}}$  only system. Presumably the dissociation of our carrier system relates to initial disruption of Ad/ $\beta\text{CD}$  interactions ( $k_d = 4 \times 10^{-3} \text{ s}^{-1}$ )<sup>61</sup> and, once in solution, the multivalency of the  $V_{\text{HH}}:\text{Ni(II)}:(\text{NTA-Ad})_3$  will be lost, followed by the eventual dissociation of the growth factor from the  $V_{\text{HH}}$  fragments. SPR studies were also performed in the case of following the one-pot assembly scheme. After recording a baseline by continuously flowing a solution of  $0.1 \text{ mM}$  HEG-Ad, the flow was switched to a solution of hBMP-6 in the presence of different concentrations of  $V_{\text{HH}}$  (and  $\text{Ni(II)}:\text{NTA-Ad}$ ) while monitoring the SPR intensity (Figure 4c). When a  $50 \text{ nM}$  solution of hBMP-6 was used in the presence of a  $2 \mu\text{M}$  solution of  $V_{\text{HH}}$ , an increase in the SPR resonant angle was observed when compared to the case when a  $2 \mu\text{M}$  solution of  $V_{\text{HH}}:\text{Ni(II)}:\text{NTA-Ad}$  was flown without hBMP-6 (Figure 4c, short dashed versus dotted line). A similar observation was made when using a  $210 \text{ nM}$  solution of hBMP-6 in the presence of a  $5 \mu\text{M}$  solution of  $V_{\text{HH}}$  (Figure 4c, long dashed versus dot-dashed line). When a solution containing only hBMP-6 was flown, no increase in the SPR intensity was observed, indicating that non-specific interactions between hBMP-6 and the background surface are insignificant (Figure, 4c, straight line). These results confirm that hBMP-6 can specifically be loaded onto the  $V_{\text{HH}}$  carrier system, in agreement with MST and ELISA studies, while in addition hBMP-6 can be immuno-stained on the  $V_{\text{HH}}$  carrier system, presumably indicating that the active conformation of the growth factor is maintained.

**Cell Response.** To explore the bioactivity of the supramolecularly loaded hBMP-6 surfaces, the induction of alkaline phosphatase (ALP) was measured as early marker of osteogenic differentiation of KS483 mouse progenitor cells.<sup>62, 63</sup> Cell line KS483 is a mesenchymal

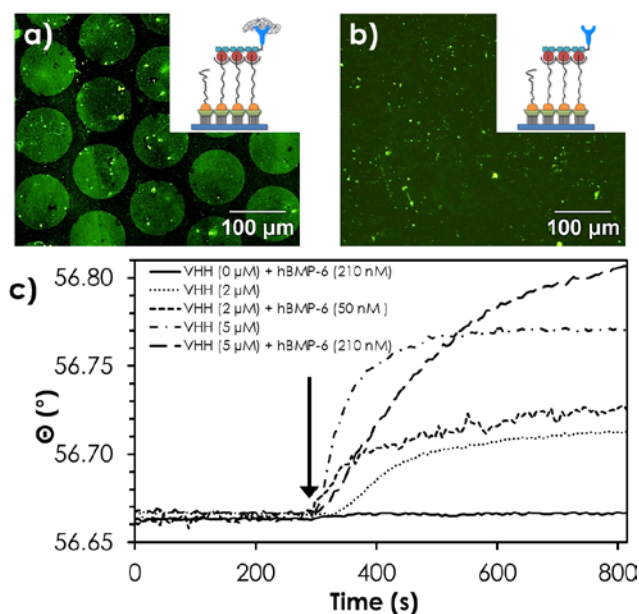


**Figure 4.** Fluorescence microscopy images after immunostaining the patterned (dots of  $100 \mu\text{m}$  in diameter and spaced by  $20 \mu\text{m}$ ) supramolecular  $V_{\text{HH}}$  carrier systems a) loaded and b) unloaded with hBMP-6. Insets show a scheme representing each assembly c) SPR sensograms of flowing  $V_{\text{HH}}:\text{Ni(II)}:\text{NTA-Ad}$  with/without hBMP-6 as indicated in the legend over a  $\beta\text{CD}$  slide. The solutions were pre-mixed for at least 30 min before injection (arrow) in the presence of  $0.1 \text{ mM}$  of HEG-Ad.

precursor cell line that differentiates into osteoblasts during a 1-3 week culture period when cultured under osteogenesis-inducing conditions.<sup>62, 63</sup> While mature human and mouse BMP-6 share 96% amino acid identity and their cross reactivity with mouse and human BMP receptors, the use of a murine cell line, such as KS483, is suitable to assess the ability of hBMP-6 to initiate differentiation into mineralizing osteoblasts.<sup>62, 63</sup> After cell culturing on fully coated (non-patterned) hBMP-6 surfaces for 7 days a Live/Dead assay showed negligible cytotoxicity (Figure 5c). From a series of fully coated hBMP-6 surfaces and controls, the ALP activity was measured and normalized to the DNA content. Data is expressed as relative induction in comparison to a bare glass substrates (Figure 5a) or to a layer of immobilized  $V_{\text{HH}}$  (Figure 5b). When hBMP-6 was loaded onto the  $V_{\text{HH}}$  carrier system in a step-by-step assembly process, the ALP activity was 6-fold higher in comparison to the case when  $V_{\text{HH}}$  functionalized surfaces were used that lacked hBMP-6 (Figure 5a). In contrast, ALP activity was enhanced at best 2-fold when soluble hBMP-6 was simply adsorbed to surfaces that lack the  $V_{\text{HH}}$  carrier system or glass only. No induction of ALP activity was observed for the  $V_{\text{HH}}$  carrier system without hBMP-6. These results confirm that presenting hBMP-6 through  $V_{\text{HH}}$  functionalized surfaces show the best differentiation response as assessed by measuring ALP activity after 7 days of differentiation.<sup>61-63</sup> This increase in differentiation response could be attributed to the activity of hBMP-6

only. When hBMP-6 was partly denatured at 95 °C after loading the V<sub>H</sub>H carrier system, the ALP activity was significantly decreased. An ELISA experiment was performed to determine the amount of surface loaded hBMP-6 on the V<sub>H</sub>H carrier system, which was prepared following the step-by-step procedure. The released amount of hBMP-6 after 7 days was determined to be 142 ± 17 ng. This result may give reason to the higher ALP activity observed for hBMP-6 loaded surfaces when compared with reference experiments on glass and on substrates functionalized with V<sub>H</sub>H in which 100 ng of hBMP-6 was added to the cell culture medium. However, when cells were seeded on hBMP-6 loaded surfaces that were prepared following the one-pot assembly procedure using a solution of 100 ng of hBMP-6 and 0.5 μM V<sub>H</sub>H·Ni(II)·NTA-Ad (1:5:5), a 6-fold relative induction of the ALP production was observed with respect to the case when hBMP-6 was left out of the assembly solution to give V<sub>H</sub>H-only surfaces (Figure 5b). These results show that irrespective of the assembly procedure, biologically relevant amounts of hBMP-6 can be functionally delivered to cells through the supramolecular V<sub>H</sub>H carrier system.

## Conclusion

We demonstrated that employing V<sub>H</sub>H fragments gives access to capturing growth factors with high affinities while their recombinant production is convenient and gives entry to modification through genetic engineering. While V<sub>H</sub>H fragments resemble human antibodies, immune response is presumably negligible as opposed to other peptide systems.<sup>23-25</sup> Our results show that irrespective of the assembly procedure, biologically relevant amounts of hBMP-6 can be functionally loaded onto the supramolecular V<sub>H</sub>H carrier system and successively delivered to cells. We show that growth factors can be sequestered to the V<sub>H</sub>H carrier system indicating that locally excreted growth factors can possibly be bound to the surface assisted by V<sub>H</sub>H. Introduction of supramolecular coupling strategies offers additional opportunities to modulate release profiles through variation of binding strengths<sup>40</sup> and dissociation rates or combination of supramolecular with covalent strategies.<sup>65</sup> Using oriented V<sub>H</sub>H fragments on surfaces to carry growth factors provides a novel opportunity to incorporate growth factors in various systems such as hydrogels or scaffolds<sup>45</sup> and we believe that this will open new ways to develop instructed biomaterials.

## ASSOCIATED CONTENT

**Supporting Information.** Experimental details. This material is available free of charge via the Internet at <http://pubs.acs.org>.

## AUTHOR INFORMATION

### Corresponding Authors

\* [j.huskens@utwente.nl](mailto:j.huskens@utwente.nl); [h.b.c.karperien@utwente.nl](mailto:h.b.c.karperien@utwente.nl);  
[p.jonkheijm@utwente.nl](mailto:p.jonkheijm@utwente.nl).

## ACKNOWLEDGMENTS

Work by J.C-D., E.R. and E.L. was funded by Project P2.02 OAccontrol of the research program of the BioMedical Materials Institute, co-funded by the Dutch Ministry of Economic Affairs. Work by J.v.W was funded by Nanonext NL (o6C.11). The work by P.J. was funded by a starting grant from the European Research Council (no 259183 Sumoman).

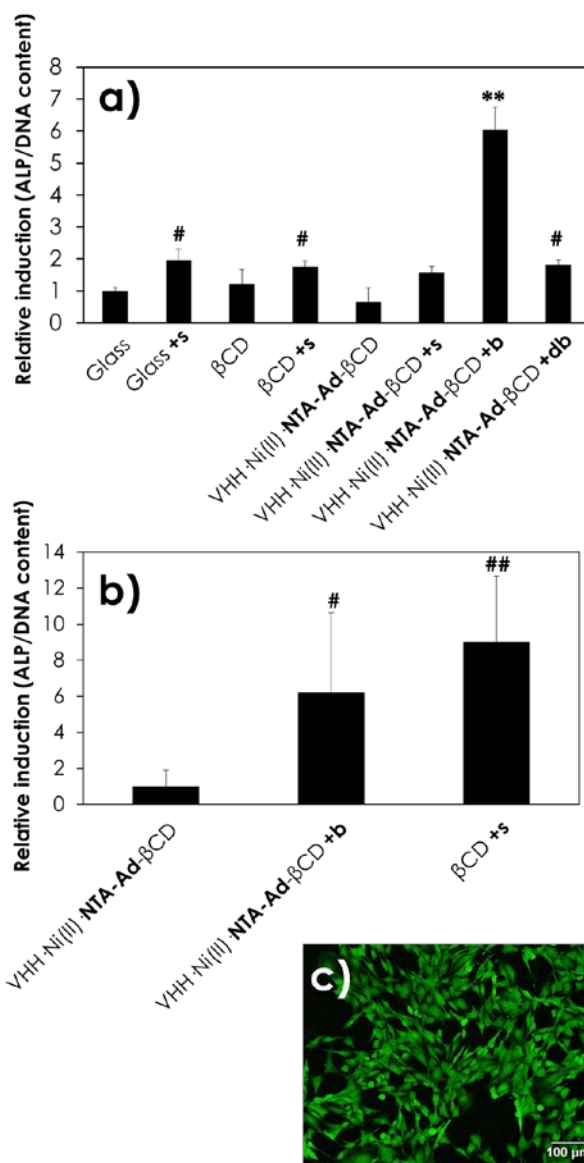


**Figure 5.** ALP activity normalized by the total DNA content of KS483 cells after 7 days of culture, expressed as relative induction with respect to a) a glass control following a step-by-step assembly procedure or to b) a supramolecular V<sub>H</sub>H carrier system following a one-pot assembly procedure. Notation on x-axis: ‘s’ represents soluble hBMP-6 supplemented to the cell medium; ‘b’ represents hBMP-6 bound to the carrier system (fully coated) ; ‘db’ represents hBMP-6 denatured at high temperature upon loading the carrier system (fully coated). #  $p < 0.05$  compared to V<sub>H</sub>H·Ni(II)·NTA-Ad, ##  $p < 0.01$  compared to V<sub>H</sub>H·Ni(II)·NTA-Ad and \*\*  $p < 0.01$  compared to all cases. c) Live-dead assay showing KS483 cells seeded on supramolecular V<sub>H</sub>H carrier system loaded with hBMP-6 (fully coated).

## REFERENCES

- (1) Boden, S. D.; Kang, J.; Sandhu, H.; Heller, J. G., *Spine* **2002**, *27*, 2662.
- (2) Takeshita, S.; Zheng, L. P.; Brogi, E.; Kearney, M.; Pu, L. Q.; Bunting, S.; Ferrara, N.; Symes, J. F.; Isner, J. M. *J. Clin. Invest.* **1994**, *93*, 662.
- (3) Takeshita, S.; Pu, L. Q.; Stein, L. A.; Sniderman, A. D.; Bunting, S.; Ferrara, N.; Isner, J. M.; Jeffrey, M.; Symes, J. F. *Circulation* **1994**, *90*, 228.
- (4) Baumgartner, I.; Pieczek, A.; Manor, O.; Blair, R.; Kearney, M.; Walsh, K.; Isner, J. M. *Circulation* **1998**, *97*, 1114.
- (5) Hendel, R. C.; Henry, T. D.; Rocha-Singh, K.; Isner, J. M.; Kereiakes, D. J.; Giordano, F. J.; Simons, M.; Bonow, R. O. *Circulation* **2000**, *101*, 118.
- (6) Lee, C. H.; Cook, J. L.; Mendelson, A.; Moiola, E. K.; Yao, H.; Mao, J. J. *The Lancet* **2010**, *376*, 440.
- (7) Yancopoulos, G.D.; Davis, S.; Gale, N.W.; Rudge, J.S.; Wiegand, S.J.; Holash, J. *Nature* **2000**, *407*, 242.
- (8) Boonthekul, T.; Mooney, D.J. *Curr. Opin. Biotechnol.* **2003**, *14*, 559.
- (9) Patterson, J.; Martino, M.M.; Hubbell, J.A. *Materials Today* **2010**, *13*, 14.
- (10) Boudou, T.; Crouzier, T.; Ren, K.; Blin, G.; Picart, C. *Adv. Mater.* **2010**, *22*, 441.
- (11) Cabanas-Danés, J.; Huskens, J.; Jonkheijm, P. *J. Mater. Chem. B* **2014**, *2*, 2381.
- (12) Murray, J.; Brown, L.; Langer, R. *Cancer Drug Delivery* **1984**, *1*, 119.
- (13) Edelman, E. R.; Mathiowitz, E.; Langer, R.; Klagsbrun, M. *Biomaterials* **1991**, *12*, 619.
- (14) Gombotz, W. R.; Pettit, D. K. *Bioconjugate Chem.* **1995**, *6*, 332.
- (15) Mahoney, M. J.; Saltzman, W. M. *Proc. Natl. Acad. Sci. U. S. A.* **1999**, *96*, 4536.
- (16) Lee, K. Y.; Peters, M. C.; Anderson, K. W.; Mooney, D. J. *Nature* **2000**, *408*, 998.
- (17) Richardson, T. P.; Peters, M. C.; Ennett, A. B.; Mooney, D. J. *Nat. Biotechnol.* **2001**, *19*, 1029.
- (18) Crouzier, T.; Fourel, T.; Boudou, T.; Albigès-Rizo, C.; Picart, C. *Adv. Mater.* **2011**, *23*, 1111.
- (19) Crouzier, T.; Ren, K.; Nicolas, K.; Roy, C.; Picart, C. *Small* **2009**, *5*, 598.
- (20) Bastings, M. M. C.; Koudstaal, S.; Kieltyka, R. E.; Nakano, Y.; Pape, A. C. H.; Feyen, D. A. M.; van Slochteren, F. J.; Doevendans, P. A.; Sluijter, J. P. G.; Meijer, E. W.; Chamuleau, S. A. J.; Dankers, P. Y. W. *Adv. Healthcare Mater.* **2013**, *3*, 70.
- (21) Wylie, R. G.; Ahsan, S.; Aizawa, Y.; Maxwell, K. L.; Morshead, C. M.; Shoichet, M. S. *Nat. Mater.* **2011**, *10*, 799.
- (22) Nguyen, T. H.; Kim, S.-H.; Decker, C. G.; Wong, D. Y.; Loo, J. A.; Maynard, H. D. *Nat. Chem.* **2013**, *5*, 221.
- (23) Wesolowski, J.; Alzogaray, V.; Reyelt, J.; Unger, M.; Juarez, K.; Urrutia, M.; Cauerhff, A.; Danquah, W.; Rissiek, B.; Scheuplein, F.; Schwarz, N.; Adriouch, S.; Boyer, O.; Seman, M.; Licea, A.; Serreze, D.; Goldbaum, F.; Haag, F.; Koch-Nolte, F. *Med. Microbiol. Immunol.* **2009**, *198*, 157.
- (24) Huang, L.; Muyltermans, S.; Saerens, D. *Expert Rev. Mol. Diagn.* **2010**, *10*, 777.
- (25) de Marco, A. *Microb. Cell Fact.* **2011**, *10*, 44.
- (26) Wong, L. S.; Khan, F.; Micklefield, J. *Chem. Rev.* **2009**, *109*, 4025.
- (27) Jonkheijm, P.; Weinrich, D.; Schroeder, H.; Niemeyer, C.M.; Waldmann, H. *Angew. Chem. Int. Ed.* **2008**, *47*, 9618.
- (28) Aida, T.; Meijer, E. W.; Stupp, S. I. *Science* **2012**, *335*, 813.
- (29) Mager, M. D.; LaPointe, V.; Stevens, M. M. *Nat. Chem.* **2011**, *3*, 582.
- (30) Rybtschinski, B. *ACS Nano* **2011**, *5*, 6791.
- (31) H. W. Jun, V. Yuwono, S. E. Paramonov, J. D. Hartgerink, *Adv. Mater.* **2005**, *17*, 2612.
- (32) Nallur, S. K. M.; Voskuhl, J.; Bultema, J. B.; Boekema, E. J.; Ravoo, B. *Angew. Chem. Int. Ed.* **2011**, *50*, 9747.
- (33) Lee, D.-W.; Park, K. M.; Banerjee, M.; Ha, S. H.; Lee, T.; Suh, K.; Paul, S.; Jung, H.; Kim, J.; Selvapalam, N.; Ryu, S. H.; Kim, K. *Nat. Chem.* **2011**, *3*, 154.
- (34) Kim, C.; Agasti, S. S.; Zhu, Z.; Isaacs, L.; Rotello, V. M., *Nat. Chem.* **2010**, *2*, 962.
- (35) Meyer, R.; Niemeyer, C.M. *Small*, **2011**, *7*, 3211.
- (36) Dankers, P. Y. W.; Harmsen, M. C.; Brouwer, L. A.; Luyn, M. J. A.; Kreijger, E. W. *Nat. Mater.* **2005**, *4*, 568.
- (37) Krogman, K. C.; Lowery, J. L.; Zacharia, N. S.; Rutledge, G. C.; Hammond, P. T. *Nat. Mater.* **2009**, *8*, 512.
- (38) Shah, R. N.; Shah, N. A.; Del Rosario Lim, M. M.; Hsieh, C.; Nuber, G.; Stupp, S. I. *Proc. Natl. Acad. Sci. U. S. A.* **2010**, *107*, 3293.
- (39) Liu, Y.; Wang, H.; Kamei, K. I.; Yan, M.; Chen, K.-J.; Yuan, Q.; Shi, L.; Lu, Y.; Tseng, H.-R. *Angew. Chem. Int. Ed.* **2011**, *50*, 3058.
- (40) Yang, L.; Gómez-Casado, A.; Young, J. F.; Nguyen, N. D.; Cabanas-Danés, J.; Huskens, J.; Brunsveld, L.; Jonkheijm, P. *J. Am. Chem. Soc.* **2012**, *134*, 19199.
- (41) González-Campo, A.; Brasch, M.; Uhlenheuer, D.; Gómez-Casado, A.; Yang, L.; Brunsveld, L.; Huskens, J.; Jonkheijm, P. *Langmuir* **2012**, *28*, 16364.
- (42) Tian, F.; Cziferszky, M.; Jiao, D.; Wahlström, K.; Geng, J.; Scherman, O. A. *Langmuir* **2011**, *27*, 1387.
- (43) An, Q.; Brinkmann, J.; Huskens, J.; Krabbenborg, S.; de Boer, J.; Jonkheijm, P. *Angew. Chem. Int. Ed.* **2012**, *51*, 12233.
- (44) Neiryneck, P.; Brinkmann, J.; An, Q.; van der Schaft, D.; Gustav Milroy, L.; Jonkheijm, P.; Brunsveld, L. *Chem. Commun.* **2013**, *49*, 3679.
- (45) Boekhoven, J.; Rubert Pérez, C. M.; Sur, S.; Worthy, A.; Stupp, S. I. *Angew. Chem. Int. Ed.* **2014**, *52*, 12077.
- (46) Park, K. M.; Yang, J.-A.; Jung, H.; Yeom, J.; Park, J. S.; Park, K.-H.; Hoffman, A. S.; Hahn, S. K.; Kim, K. *ACS Nano* **2012**, *6*, 2960.
- (47) Brinkmann, J.; Cavatorta, E.; Sankaran, S.; Schmidt, B.; van Weerd, J.; Jonkheijm, P. *Chem. Soc. Rev.* **2014**, *43*, 4449-69.
- (48) Vukicevic, S.; Grgurevic, L. *Cytokine Growth Factor Rev.* **2009**, *20*, 441.
- (49) Li, R. H.; Wozney, J. M. *Trends in Biotechnol.* **2001**, *19*, 255.
- (50) Kemmis, C. M.; Vahdati, A.; Weiss, H. E.; Wagner, D. R. *Biochem. Biophys. Res. Commun.* **2010**, *401*, 20.
- (51) van der Linden, R. H. J.; Frenken, L. G. J.; de Geus, B.; Harmsen, M. M.; Ruuls, R. C.; Stok, W.; de Ron, L.; Wilson, S.; Davis, P.; Verrips, C. T. *Biochim. Biophys. Acta, Protein Struct. Mol. Enzymol.* **1999**, *1431*, 37.
- (52) Spinelli, S.; Frenken, L. G. J.; Hermans, P.; Verrips, T.; Brown, K.; Tegoni, M.; Cambillau, C. *Biochemistry* **2000**, *39*, 1217.
- (53) De Genst, E.; Silence, K.; Decanniere, K.; Conrath, K.; Loris, R.; Kinne, J. r.; Muyltermans, S.; Wyns, L. *Proc. Natl. Acad. Sci. U.S.A.* **2006**, *103*, 4586.
- (54) González-Campo, A.; Eker, B.; Gardeniers, H.J.G.E.; Huskens, J.; Jonkheijm, P. *Small* **2012**, *8*, 3531.
- (55) Ludden, M. J. W.; Mulder, A.; Schulze, K.; Subramaniam, V.; Tampé, R.; Huskens, J. *Chem. Eur. J.* **2008**, *14*, 2044
- (56) Ludden, M. J. W.; Mulder, A.; Tampé, R.; Reinhoudt, D. N.; Huskens, J. *Angew. Chem. Int. Ed.* **2007**, *46*, 4104.
- (57) Lata, S.; Reichel, A.; Brock, R.; Tampé, R.; Piehler, J. *J. Am. Chem. Soc.* **2005**, *127*, 10205.
- (58) De, M.; Rana, S.; Rotello, V. M. *Macromol. Biosci.* **2009**, *9*, 174.
- (59) Voskuhl, J.; Brinkmann, J.; Jonkheijm, P. *Curr. Opin. Chem. Biol.* **2014**, *18*, 1-7.

- 1 (60) Gomezcasado, A.; Dam, H.H.; Yilmaz, D.; Florea, D.;  
2 Jonkheijm, P.; Huskens, J. *J. Am. Chem. Soc.* **2011**, *133*, 10849.  
3 (61) Nakamura, I.; Makino, A.; Ohmae, M.; Kimura, S. *Macromol.*  
4 *Biosci.* **2010**, *10*, 1265.  
5 (62) van der Horst, G.; van Bezooijen, R.L.; Deckers, M.M.L.;  
6 Hoogendam, J.; Visser, A.; Löwik, C.W.G.M.; Karperien, M. *Bone*,  
7 **2002**, *31*, 661-9.  
8 (63) van der Horst, G.; van der Werf, S. M.; Farih-Sips, H.; van  
9 Bezooijen, R. L.; Löwik, C. W.G. M.; Karperien, M. *J. Bone Min.*  
10 *Res.* **2005**, *20*, 1867.  
11 (64) Tsai, M.-T.; Li, W.-J.; Tuan, R. S.; Chang, W. H. *J. Orthop.*  
12 *Res.* **2009**, *27*, 1169.  
13 (65) Wasserberg, D.; Nicosia, C.; Tromp, E. E.; Subramaniam, V.;  
14 Huskens, J.; Jonkheijm, P. *J. Am. Chem. Soc.* **2013**, *135*, 3104.  
15  
16  
17  
18  
19  
20  
21  
22  
23  
24  
25  
26  
27  
28  
29  
30  
31  
32  
33  
34  
35  
36  
37  
38  
39  
40  
41  
42  
43  
44  
45  
46  
47  
48  
49  
50  
51  
52  
53  
54  
55  
56  
57  
58  
59  
60

## TOC GRAPHIC

